

# A New RBF Classifier for Buried Tag Recognition

Larbi Beheim, Adel Zitouni and Fabien Belloir

CRéSTIC

(Centre de Recherche en Sciences et Technologies de l'Information et la Communication)

University of Reims Champagne-Ardenne

Campus du Moulin de la Housse, B.P. 1039,

51687 Reims Cedex 2, France

**Abstract.** This article presents noticeable performances improvement of an RBF neural classifier. Based on the Mahalanobis distance, this new classifier increases relatively the recognition rate while decreasing remarkably the number of hidden layer neurons. We obtain thus a new very general RBF classifier, very simple, not requiring any adjustment parameter, and presenting an excellent ratio performances/neurons number. A comparative study of its performances is presented and illustrated by examples on real databases. We present also the recognition improvements obtained by applying this new classifier on buried tag.

## 1 Introduction

The radial basic functions neural net (RBF) has become, for these last years, a serious alternative to the traditional Multi-Layer Perceptron network (MLP) in the multidimensional approximation problems. RBF Network was employed since the Seventies under the name of potential functions and it is only later than [1] and [2] rediscovered this particular structure in the neuronal form. Since, this type of network profited from many theoretical studies such as [3], [4] and [5]. In pattern recognition, RBF network is very attractive because its locality property allows discriminating complex classes such as nonconvex ones.

We consider in this article the Gaussian RBF classifier of which each  $m$  output  $s_j$  is evaluated according to the following formula:

$$s_j(X) = \sum_{l=1}^{N_h} w_{lj} \varphi_l(X) = \sum_{l=1}^{N_h} w_{lj} \exp \left\{ -\frac{1}{2} (X - C_l)^T \Sigma_l^{-1} (X - C_l) \right\} \quad (1)$$

Where  $X = [x_1 \dots x_n]^T \in \mathbb{R}^N$  is a prototype to be classified,  $N_h$  represents the total number of hidden neurons. Each one of these nonlinear neurons is characterized by a center  $C_l \in \mathbb{R}^N$  and a covariance matrix  $\Sigma_l$ .

From a training set  $S_{train} = \{X_p, \omega_p\}$ ,  $p=1 \dots N$  made up of prototypes couples  $X_p$  and its membership class  $\omega_p \in \{1, \dots, m\}$ , the supervised training problem of RBF classifier amounts determining his structure, i.e. the number of hidden neurons  $N_h$  and the

different parameters intervening in the equation of outputs (1). Whereas these parameters can be calculated by different heuristics, the estimate of  $Nh$  is often delicate. For that, many methods were developed among which we can quote [6], [7] and [8]. These methods generally require a very significant load of calculation without however guaranteeing significant performances. Moreover, they often require a certain number of parameters that must be fixed a priori and optimized for a particular problem. So these methods cannot be applied systematically and without particular precautions to any type of classification problem. The article [9] proposed a very simple algorithm, which generates automatically a powerful RBF network without any optimization nor introduction of parameters fixed a priori. Indeed, the algorithm automatically selects the number of the hidden layer neurons. Although this network is characterized by its great simplicity, it presents a major limitation however owing to the fact that it requires a rather significant number of neurons in the hidden layer. This limitation makes it very heavy and requiring very significant training times for the very large databases.

In this article we propose a solution to this problem by introducing the Mahalanobis distance. We thus obtain a new very general, very simple RBF network and presenting an excellent performances/neurons number ratio. We present also the recognition improvements obtained by applying this new classifier on buried tag coding system.

The organization of the article is as follows: In section 2, we describe the new RBF network and we present the associated algorithm. Its operation is illustrated for an example on an artificial database. In section 3, we study its properties and in section 4 its performances on real problems. Finally, we present results obtained by application of this classifier on buried tag coding system.

## 2 Algorithm

In this section, we describe the principle of construction proposed as well as the algorithm allowing its implementation. We illustrate then his operation in a problem of classification including two classes of which one is not convex.

### 2.1 Principle

The principle of the algorithm rests on [9]. According to the exponential nature of the functions  $\varphi_i(\cdot)$  of each hidden neuron, the activation state of each one of them decrease quickly when the vector of entry  $X$  moves away from the neuron center. So only an area of the entry space centered in  $C_i$  will provide a significantly non-null activation state. Contrary to [9], our algorithm regards this area as a hyperellipsoide centered in  $C_i$ . Indeed, the use of the Mahalanobis distance makes it possible to take into account the statistical distribution of the prototypes around the centers  $C_i$  and thus a better representation of classes shape. Our algorithm proposes to divide a non-

convex class into a set of hyperellipsoids called clusters. Each cluster corresponds to a hidden neuron and it is characterized thus by a center placing it in the entry space, a matrix of covariance indicating the privileged directions and a width calculating the extension of the hyperellipsoide. In the continuation, we will not make any more the distinction between a neuron and a cluster.

## 2.2 Description

Before describing the construction algorithm of the RBF classifier, we will introduce some notations used thereafter. At the  $k^{th}$  iteration, we define  $C_{ij}^{(k)}$  like the  $i^{th}$  center ( $i=1 \dots m^{(k)}_j$ ) characterizing the class  $\Omega_j$ . With each center a covariance matrix is associated  $\Sigma_{ij}^{(k)}$  and a width  $L_{ij}^{(k)}$ . We note  $H_{ij}^{(k)}$  the hyperellipsoide of center  $C_{ij}^{(k)}$  such as:

$$H_{ij}^{(k)} = \left\{ X_p \in \Omega_j, (X_p - C_{ij}^{(k)})^T \Sigma_{ij}^{(k)-1} (X_p - C_{ij}^{(k)}) < L_{ij}^{(k)} \right\} \quad (2)$$

Each class is characterized by the area  $R_j^{(k)}$  defined as the union of all the hyperellipsoids  $H_{ij}^{(k)}$  ( $i=1 \dots m^{(k)}_j$ ).

We will also use the distance  $d(R_j^{(k)}, X)$  between a point  $X \in \Omega_j$  and its associated area  $R_j^{(k)}$ . This one is defined as the Mahalanobis distance between  $X$  and the nearest center  $C_{ij}^{(k)}$  of  $R_j^{(k)}$ :

$$d(R_j^{(k)}, X) = \min_{i=1 \dots m^{(k)}_j} (X - C_{ij}^{(k)})^T \Sigma_{ij}^{(k)-1} (X - C_{ij}^{(k)}) \quad (3)$$

Step 0 (initialization): For  $k=0$ , we define  $m$  clusters whose centers correspond to the gravity centers of different classes  $\Omega_j$  ( $N_j$  is the element number of  $\Omega_j$ ):  
 $m^{(0)}_j=1$  and

$$C_{1j}^{(0)} = \frac{1}{N_j} \sum_{X_p \in \Omega_j} X_p, j=1 \dots m \quad (4)$$

$$\Sigma_{1j}^{(0)} = \frac{1}{N_j - 1} \sum_{X_p \in \Omega_j} (X_p - C_{1j}^{(0)}) (X_p - C_{1j}^{(0)})^T, j=1 \dots m \quad (5)$$

Step 1 (adjustment of the widths): The width  $L_{ij}^{(k)}$  relating to the center  $C_{ij}^{(k)}$  is defined like the half of Mahalanobis distance between this center and the nearest center of another class:

$$L_{ij}^{(k)} = \frac{1}{2} \min_{\substack{t \neq j, s=1 \dots m^{(k)}_t \\ i=1 \dots m^{(k)}_j, j=1 \dots m}} (C_{ij}^{(k)} - C_{st}^{(k)})^T \Sigma_{ij}^{(k-1)-1} (C_{ij}^{(k)} - C_{st}^{(k)}) \quad (6)$$

Step 2 (search for an orphan point): We seek a point  $X_i \in S_{train}$  not belonging to its associated area  $R_{oi}^{(k)}$  and most distant from this one:

$$X_i = \arg \max_{X_s \in S_{train}} d(R_{\omega_s}^{(k)}, X_s) \quad (7)$$

If such a point does not exist, go to the step 5.

Step 3 (creation of a new center): Point  $X_i$  found at step 2 becomes a new center composing the class  $\Omega_{\omega_i}$  :

$$m_j^{(k)} = m_j^{(k)} + 1 \quad C_{m_j^{(k)}, j}^{(k)} = X_i \quad (8)$$

Step 4 (Reorganization of the centers): The K-means clustering algorithm is applied to the points of  $S_{train}$  pertaining to the class  $\Omega_{\omega_i}$  in order to distribute as well as possible the  $m_j^{(k)}$  centers. Calculate the new covariance matrices:

$$\Sigma_{ij}^{(k)} = \frac{1}{\text{Card}(H_{ij}^{(k)}) - 1} \sum_{X_p \in H_{ij}^{(k)}} (X_p - C_{ij}^{(k)})(X_p - C_{ij}^{(k)})^T \quad (9)$$

Do  $k=k+1$  and go to the step 1.

Step 5 (determination of the weights): The weights matrix  $W^*$  which minimizes an error function, here selected as the sum square errors of classification, and is given by:

$$W^* = \left[ H^T H \right]^{-1} H^T T \quad (10)$$

where  $H$  and  $T$  are the matrices respectively gathering the activation function stats and the target outputs. These last are fixed at 1 when they correspond to the class of the point and 0 elsewhere.

### 2.3 Discussion

The initialization of the algorithm (step 0) could have proceeded by the random placement of a number of given centers. This technique is very current in the definition of an RBF network. The fact of choosing the initial centers as gravity centers of the points  $X_p$  makes it possible to avoid this unforeseeable character and provides moreover the number of these centers. Thus, the result of the algorithm depends only on the composition of the training data. In certain cases where the classes are non convex, it may be that the gravity center of a class is inside another class. This situation is not prejudicial for the algorithm since this center will be moved during following iterations. The covariance matrix corresponding to each center is obtained from the associated training data. We will further see that other definitions of this matrix can give different results. In step 1,  $L_{ij}^{(k)}$  is defined relatively to the minimal distance between the center  $C_{ij}^{(k)}$  and centers of another class. This means that a partial covering between the clusters of the same class is authorized. From a practical point of view, that makes it possible to optimize the space occupation of the attributes by the various zones of receptivity and thus to reduce the number of clusters necessary to compose each class. The elliptic volume covered by each cluster is maximal without

encroaching on neighboring classes. In step 2, the fact of choosing the furthest point from the region  $R^{(k)}_j$  makes it possible to improve the effectiveness of the algorithm of K-means clustering used at step 4. It should be noted that this one relates only to the centers constituting the same class since the other centers did not change a position. It guarantees moreover a fast development of this area. In the network training (step 5), the target outputs are fixed arbitrarily at 1 when they correspond to the class of the point and 0 elsewhere. The motivation of this practice is artificially to create a brutal fall of the membership degree at the geometrical border of the class.

After  $k$  iterations, all the points of Strain belong to a cluster, the algorithm generated  $m+k$  clusters defining as many subclasses. The RBF network thus built comprises then  $Nh=m+k$  hidden neurons. We can note that the algorithm converges necessarily. Indeed, in the "worst case" where none the classes is separable, there will be creation of a cluster for each point of Strain.

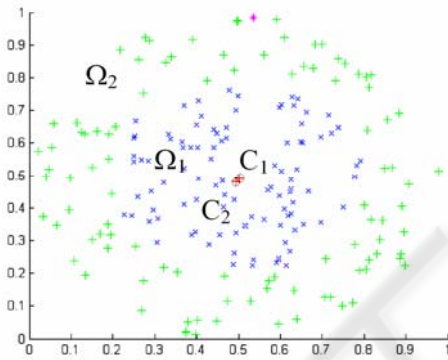


**Fig. 1.** Algorithm initialization.

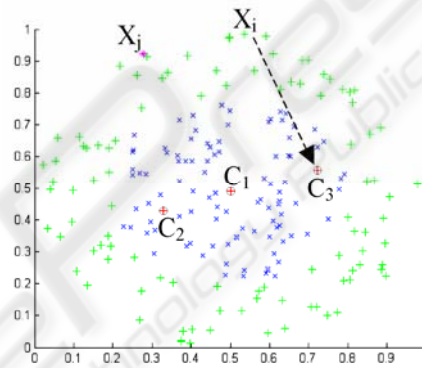


**Fig. 2.** 1st iteration of the algorithm.

## 2.4 Illustration of operation

We will illustrate the significant phases of the algorithm on a classification problem of two concentric classes from the databases of "ELENA" project [10] [11]. This base makes it possible to determine the capacity of a classifier to separate two classes not overlapping but of which one is included in the second.

The RBF network comprises 2 inputs and 2 outputs. The figure 1a shows the 2 initial centers  $\{C_1, C_2\}$  obtained following step 0. We can see that the two centers are almost confused. Each cluster induced is delimited by an ellipse of the width calculated at step 1. Obviously, the cluster of center  $C_2$  is not sufficient to entirely represent the class  $\Omega_2$ . This one thus will be subdivided in several subclasses. With the first iteration of the algorithm, the point noted  $X_i$  on the figure 2 is the furthest from the center  $C_2$  and is out of the corresponding cluster. The addition of a new center compared to this point led, after application of the K-means, to the new distri-

bution  $\{C_1, C_2, C_3\}$  illustrated by the figure 2. The point  $X_t$  is now the furthest from the center  $C_3$  on this figure. After application of the K-means on this new configuration one leads to the figure 3. After 4 iterations, the 2 classes are discriminated perfectly and the neuronal classifier comprises a total of 5 neurons (see figure 4). After having determined the number of centers necessary and their positions, the weights of the network are calculated according to equation of step 5. The algorithm thus manages to separate the two classes with only 5 neurons against 108 neurons for the old algorithm using the Euclidean distance and with a slightly higher rate of recognition: 98% against 97.7% for the old RBF.

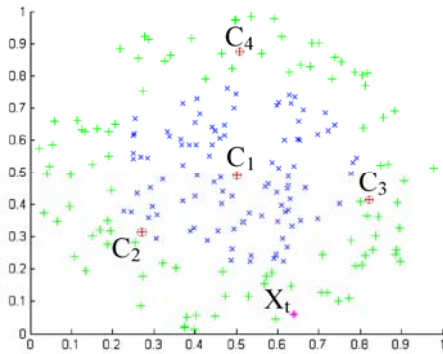


**Fig. 3.** 2nd iteration of the algorithm.

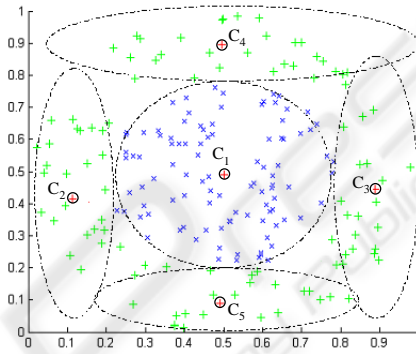


**Fig. 4.** Result of classification of the algorithm.

## 2.5 The choice of the covariance matrix

One of the limits of this classifier is the estimate of the covariance matrix. The larger the size of the clusters is and the better is the estimate of this matrix. So the calculation of this matrix can sometimes reduce the rates of recognition. To cure this problem, other calculations of this matrix can be proposed to take into account more prototypes during the estimate of this matrix.

Table 1 gives examples of calculation, errors and the corresponding number of neurons. One can see on this table that a different choice of the covariance matrix that proposed in section 2 can increase or decrease the rate error but the number of hidden neurons can only increase. But this number remains always largely lower than the number of neurons proposed by the old RBF.

**Table 1.** Error rate of the base Textures according to the choice of the matrix of covariance

Covariance Matrix <sup>a</sup>		Error(%)	Nh
$\Sigma = \text{cov}(C)$	(a)	2,90	24
$\Sigma = \text{cov}(J_i)$	(b)	1,94	3

$\Sigma=\text{cov}(Jc_i)$	(c)	1,73	858
$\Sigma=\text{cov}(J)$	(d)	0,41	22

<sup>a</sup>(a) covariance of the centers, (b) covariance of the data of each class (c) covariance of the data of each center (d) covariance of the total database.

### 3 Benchmarks

The object of this section is to evaluate the performances of the RBF classifier built by the algorithm presented in section 2. For that, we applied the classifier to various problems of classification comprising a variable number of attributes and classes and bearing from the real world situations.

#### 3.1 Pima Indians Diabetes Database

This database is from the Machine Learning database repository at the University of California, Irvine [12]. In this problem there are two classes representing results of a diabetes test given to Pima Indians. There are 8 attributes, and 768 examples, randomly partitioned into two disjoint subsets of equal size for training and testing. Table 2 presents comparative results of different classifiers (backpropagation networks, decision trees or support vector machines [13],...). For more details on methods of this table see [14].

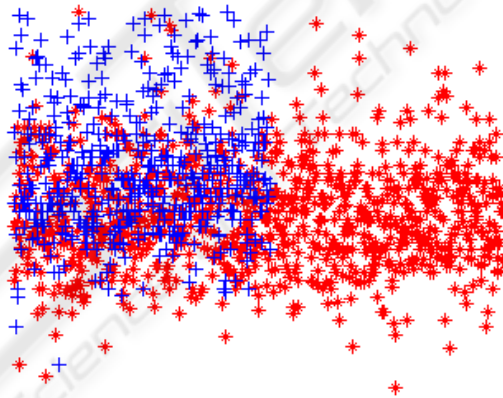


**Fig. 5.** Pima Indians database (2 first attributes)

We can see on this example, the RBF classifier gives the weakest error rate (with the Linear MSE classifier). The relatively high error rate (23%) and the number of hidden neurons (76 units) is due to the fact that this database comprises partially superimposed classes (see Figure 5).

**Table 2.** Pima Indians Database Results

Method	Error rate (%)
Linear MSE (pseudoinverse)	23
Oblique Decision Tree 8 decision nodes	24
1-1 Nearest Neighbor	30
2-3 Nearest Neighbor	25
Full covariance gaussian mixture, 1 component/class	26
Full covariance gaussian mixture, 2 component/class	29
Full covariance gaussian mixture, 3 component/class	30
Full covariance gaussian mixture, 4 component/class	31
Backprop Multilayer Perceptron 2 hidden units	25
Backprop Multilayer Perceptron 4 hidden units	24
Backprop Multilayer Perceptron 8 hidden units	29
Support Vector Machine, RBF kernel, width 1 (297 s.v.)	30
Support Vector Machine, RBF kernel, width 3 (176 s.v.)	35
Support Vector Machine, polynomial kernel, order 4 (138 s.v.)	36
Support Vector Machine, polynomial kernel, order 5 (131 s.v.)	34
MFGN 4 components	35
MFGN 6 components	32
MFGN 8 components	35
Our RBF classifier (76 hidden units)	23

### 3.2 ELENA Databases

The benchmarks carried out here are studied in detail in ELENA project [10]. The three databases result from real problems. The "Phoneme" problem relates to the speech recognition. The principal difficulty of this problem is great dissymmetry in the number of authorities of each classes. The "Iris" data is very known in the pattern recognition. To finish, the data of the "Texture" file relates to the recognition of 11 natural micro-textures such as grass, sand, paper or certain textiles. For each problem of classification, we have the results concerning the RBFM classifier generated by the algorithm proposed, the RBFM is the classical RBF classifier based on Euclidian distance and other classifiers studied in [11]. The table 3 presents results on these various problems. The performances of the RBF classifier are slightly lower than the other classifiers for the first problem. This is explained by the significant interlacing of the two classes. The algorithm generates a neuron number close to the point's number of training data and the capacities of generalization on the test set are thus very bad.

**Table 3.** Error rate (%) and hidden neuron number (Nh) on four different databases

Method	Phoneme	Iris	Texture
KNN	12.90	3.50	2.20
MLP	16.10	4.10	2.10
LVQ	17.10	6.10	3.40
	10.90	2.90	1.80
RBFE (Euclidian)	Nh=227	Nh=24	Nh=858



	10.43	1.94	0.41
RBFM (Mahalanobis)	Nh=59	Nh=3	Nh=22

The error rate of our classifier RBFM is generally the weakest for each of the last three problems. This is checked whatever the number of classes to be distinguished and the quantity of available data for the training.

We can see on this table the "compact" quality of our classifier who gives comparable error rates or even lower while minimizing the hidden neurons number Nh. So, training times are much less significant. For the "Textures" database for example, the error rate is divided by 4, while the number of hidden neurons is divided by 39. It was necessary less than two minutes to training our classifier and more than one hour for a classical RBFE classifier.

#### 4 Application in buried tag identification

The goal of our application is to detect and identify reliably different buried metallic codes with a smart eddy current sensor. Based on the principle of the induction balance, our detector measures the magnetic fields modifications emitted by a coil. These modifications are due to the presence of the metal codes buried on the top of the drains. A code is built from a succession of different metal pieces separated by empty spaces. Thus the identification of the codes allows the identification and the localization of the pipes (like water, gas,...) [15].

Several material improvements were carried out on our detector [16], but the identification of the codes always poses problems because of the similarity between the codes, the non-linearity of the answer according to the depth and the choice of a suitable coding of the signals [17]. To solve these problems, various methods of classifications were proposed. These methods are based on neural networks. Among all developed methods it is the classifier RBFE (Euclidean RBF) who gives the best results. But, these results remain insufficient for the great depths. It is for that we developed this new classifier to try to decrease rate errors and neurons number for a future integration of the classifier on programmable microchips. A comparison is made between these different methods and the new RBF classifier. For a burying depth up to 80 cm, we obtain the results given in the table 4. We can notice that the result of the new RBF classifier is better than the others, and always with less number of hidden neurons.

**Table 4.** Results of code misclassification for the 5 pattern recognition methods implemented

Classifier <sup>a</sup>	RBFM	RBFE	SOM
Error (%)	5.0	6.2	11.3
Nh	68	135	80

<sup>a</sup>RBFM=RBF based on Mahalanobis distance, RBFE= RBF based on Euclidian distance, SOM=Self Organization Map.

## 5 Conclusion

We proposed a noticeable performances improvement of a neural classifier based an RBF network. The new classifier is very general and simple. It generates automatically a powerful RBF network without any introduction of parameters fixed a priori. The number of hidden neurons is very optimized what will allow its use for the very large databases. Indeed, the new classifier obtains excellent recognition results for a variety of different databases and particularly the buried tag recognition. On this application we can also note a reduction in the error rate (relatively weak) but especially a very clear reduction in the number of hidden neurons (division by 2). This allows a notable saving of the training times necessary to the development of the system.

## References

1. D.S. Broomhead and D. Lowe, Multivariable functional interpolation and adaptive networks, *Complex Systems*, Vol.2, 1988, pp. 321-355.
2. J. Moody and C.J. Darken, Fast Learning in Networks of Locally-Tuned Processing Units. *Neural Computation*, Vol.1, 1988, pp. 281-294.
3. F. Girosi and T. Poggio, Networks and The Best Approximation Property, Technical Report C.B.I.P. No. 45, Artificial Intelligence Laboratory, Massachusetts Institute of Technology, 1989.
4. Park J. and Sandberg I.W., Universal Approximation Using Radial-Basis-Function Networks, *Neural Computation*, Vol.3, 1991, pp. 246-257.
5. M. Bianchini, P. Frasconi and M. Gori, Learning without Local Minima in Radial Basis Function Networks, *IEEE Transactions on Neural Networks*, Vol.6:3, 1995, pp. 749-756.
6. B. Fritzke, Supervised Learning with Growing Cell Structures, In *Advances in Neural Processing Systems 6*, J.C. Cowan, Tesauo G. and Alspector J. (eds.), Morgan Kaufmann, San Mateo, CA., 1994.
7. B. Fritzke, Transforming Hard Problems into Linearly Separable one with Incremental Radial Basis Function Networks, In M.J. Vand Der Heyden, J. Mrsic-Flögel and K. Weigel (eds.), *HELNET International Workshop on Neural Networks, Proceedings Volume I/II 1994/1995*, VU University Press, 1996
8. C.G. Looney, *Pattern Recognition Using Neural Network - Theory and Algorithms for Engineers and Scientists*, Oxford University Press, Oxford - New York, 1997.
9. F. Belloir, A. Fache and A. Billat, A General Approach to Construct RBF Net-Based Classifier, *Proc. of the European Symposium on Artificial Neural Networks (ESANN'99)*, April 21-23, Bruges Belgium, 1999, pp. 399-404.
10. C. Aviles-Cruz, A. Guerin-Dugué, J.L. Voz and D. Van Cappel, Deliverable R3-B1-P Task B1: Databases, Technical Report ELENA ESPRIT Basic Research Project Number 6891, June 1995.
11. F. Blayo, Y. Cheneval, A. Guerin-Dugué, R. Chentouf, C. Aviles-Cruz, J. Madrenas, M. Moreno and J.L. Voz, Deliverable R3-B4-P Task B4: Benchmarks, Technical Report ELENA ESPRIT Basic Research Project Number 6891, June 1995.
12. Merz, C.J. and Murphy, P.M. (1996). UCI Repository of machine learning databases. [<http://www.ics.uci.edu/~mllearn/MLRepository.html>]. Irvine, CA: University of California

nia,

Department of Information and Computer Science.

13. F. Friedrichs, C. Igel, Evolutionary Tuning of Multiple SVM Parameters, Proceedings of the 12th European Symposium on Artificial Neural Networks (ESANN 2004), Evere, Belgium, 2004.
14. A. Ruiz, P. E. López-de-Teruel, M. C. Garrido, Probabilistic Inference from Arbitrary Uncertainty using Mixtures of Factorized Generalized Gaussians, *Journal of Artificial Intelligence Research* 9, pp. 167-217, 1998.
15. F. Belloir, F. Klein and A. Billat, Pattern Recognition Methods for Identification of Metallic Codes Detected by Eddy Current Sensor, *Signal and Image Processing (SIP'97)*, Proceedings of the IASTED International Conference, 1997, pp. 293-297.
16. L. Beheim, A. Zitouni, F. Belloir, Problem of Optimal Pertinent Parameter Selection in Buried Conductive Tag Recognition, *Proceedings of WISP'2003, IEEE International Symposium on Intelligent Signal Processing*, Budapest (Hungary), 4-6 September 2003, pp. 87-91.
17. F. Belloir, L. Beheim, A. Zitouni, N. Liebaux, D. Placko, Modélisation et Optimisation d'un Capteur à Courants de Foucault pour l'Identification d'Ouvrages Enfouis, 3e Colloque Interdisciplinaire en Instrumentation (C2I'2004), Cachan (France), 29-30 janvier 2004.

